ACS Synthetic Biology
Cite This: ACS Synth. Biol. 2018, 7, 2074−2086
Letter
pubs.acs.org/synthbio

Birth of a Photosynthetic Chassis: A MoClo Toolkit Enabling Synthetic Biology in the Microalga *Chlamydomonas reinhardtii*

Pierre Crozet,[†,¶] Francisco J. Navarro,[‡,¶] Felix Willmund,[§,¶] Payam Mehrshahi,[‡,¶] Kamil Bakowski,[∥] Kyle J. Lauersen,[⊥] Maria-Esther Pérez-Pérez,[#] Pascaline Auroy,[▽] Aleix Gorchs Rovira,[‡] Susana Sauret-Gueto,[‡] Justus Niemeyer,[§] Benjamin Spaniol,[§] Jasmine Theis,[§] Raphael Trösch,[§] Lisa-Desiree Westrich,[§] Konstantinos Vavitsas,[∥,□] Thomas Baier,[⊥] Wolfgang Hübner,[○] Felix de Carpentier,[†] Mathieu Cassarini,[†] Antoine Danon,[†] Julien Henri,[†] Christophe H. Marchand,[†] Marcello de Mia,[†] Kevin Sarkissian,[†] David C. Baulcombe,[‡] Gilles Peltier,[▽] José-Luis Crespo,[#] Olaf Kruse,[⊥] Poul-Erik Jensen,[∥] Michael Schroda,*[,§] Alison G. Smith,*[,‡] and Stéphane D. Lemaire*[,†]

[†]Institut de Biologie Physico-Chimique, UMR 8226, CNRS, Sorbonne Université, Paris, France
[‡]Department of Plant Sciences, University of Cambridge, Cambridge, CB2 3EA, U.K.
[§]Department of Biology, Technische Universität Kaiserslautern, Kaiserslautern, 67663, Germany
[∥]Copenhagen Plant Science Centre, Department of Plant and Environmental Sciences, University of Copenhagen, Copenhagen, Denmark
[⊥]Faculty of Biology, Center for Biotechnology (CeBiTec), Bielefeld University, Bielefeld, 33615, Germany
[#]Instituto de Bioquímica Vegetal y Fotosíntesis, CSIC-Universidad de Sevilla, Sevilla, 41092, Spain
[▽]Laboratoire de Bioénergétique et Biotechnologie des Bactéries et Microalgues Cadarache, Aix Marseille University, CEA, CNRS, BIAM, Saint Paul-Lez-Durance, France
[○]Biomolecular Photonics, Department of Physics, Bielefeld University, Bielefeld, 33615, Germany

Supporting Information

ABSTRACT: Microalgae are regarded as promising organisms to develop innovative concepts based on their photosynthetic capacity that offers more sustainable production than heterotrophic hosts. However, to realize their potential as green cell factories, a major challenge is to make microalgae easier to engineer. A promising approach for rapid and predictable genetic manipulation is to use standardized synthetic biology tools and workflows. To this end we have developed a Modular Cloning toolkit for the green microalga *Chlamydomonas reinhardtii*. It is based on Golden Gate cloning with standard syntax, and comprises 119 openly distributed genetic parts, most of which have been functionally validated in several strains. It contains promoters, UTRs, terminators, tags, reporters, antibiotic resistance genes, and introns cloned in various positions to allow maximum modularity. The toolkit enables rapid building of engineered cells for both fundamental research and algal biotechnology. This work will make *Chlamydomonas* the next chassis for sustainable synthetic biology.

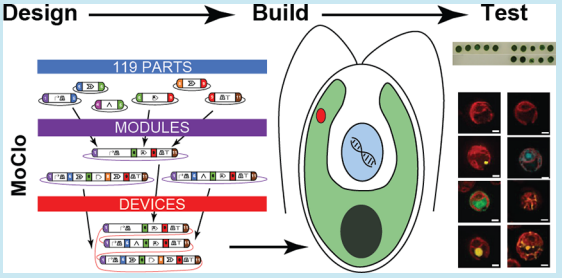

KEYWORDS: *algal biotechnology, Chlamydomonas reinhardtii, modular cloning, synthetic biology*

There is an urgent need to decarbonize the world economy due to depletion of fossil fuel reserves coupled with accumulation of greenhouse gases produced by their combustion. One alternative to the use of fossil fuels is to use photosynthetic microorganisms, such as microalgae, as green cell factories to produce fuels and chemicals from atmospheric CO_2 in a sustainable process driven by sunlight.[1,2] The fixed carbon can be redirected toward compounds that can be used in the fuel, food, cosmetic, and pharmaceutical industries, such as proteins, alcohols, alkanes, lipids, sugars, pigments or terpenes.[3−5] By contrast with land plant-based photoproduction, microalgae do not compete with agriculture and can be grown at high yields even at large scale,[4,6] including on waste streams, thus minimizing inputs.[3] The green microalga *Chlamydomonas reinhardtii* (referred to hereafter as "Chlamydomonas") has been extensively engineered for basic research and industrial biotechnology.[4,6−8] Its nuclear and

Received: June 11, 2018
Published: August 30, 2018

DOI: 10.1021/acssynbio.8b00251
ACS Synth. Biol. 2018, 7, 2074−2086

organellar genomes are sequenced and annotated, molecular biology techniques and culture conditions are highly developed, and its physiology and metabolism are well understood.[9−13] Moreover, the metabolic plasticity and cellular compartments of Chlamydomonas offer great potential for advanced metabolic engineering strategies.[14,15] Chlamydomonas has already been engineered for production of the biodiesel precursor bisabolene,[8] the terpene patchoulol,[7] and recombinant proteins as well as enzymes such as an HIV antigen[16] and xylanase.[17] Despite these proofs of concept, however, the engineering of Chlamydomonas is still slow owing to a lack of standardized resources and tools.[11] Development of the field of algal synthetic biology offers the means to enable design and construction of microalgal cells with defined and predictable properties.[18] Besides biotechnological applications, the transition from empirical to synthetic approaches also provides the opportunity to answer fundamental biological questions using new concepts and approaches based on understanding by construction rather than deconstruction.

Synthetic biology approaches, predicated on the Design−Build−Test−Learn cycle,[19] make organisms easier to engineer through the use of standardized parts and their assembly to simplify the building of designed DNA molecules.[19] Among available standards,[20] the Golden Gate Modular Cloning (MoClo) technology, based on Type IIS restriction enzymes, offers extensive standardization and allows the assembly of complex multigenic DNA from basic gene parts (e.g., promoters, CDS, terminators) in just two steps.[21,22] The method accelerates and multiplies the possibilities to permute multiple genetic elements, and makes facile the building of multigene constructs for full metabolic pathways.[23] MoClo is efficient and versatile, but relies on the intensive upfront generation of a standardized library of basic building blocks, the gene parts, that have been domesticated to remove Type IIS sites, and codon optimized for the host as appropriate. MoClo toolkits have already been developed for a few model organisms[24−29] although not yet for microalgae.

Here, we report the generation of a MoClo toolkit composed of more than 100 gene parts codon-optimized for the Chlamydomonas nuclear genome. These genetic parts were designed to provide maximum modularity to end-users, and to facilitate the development of engineered strains for fundamental and green biotechnological applications, through iterative design and testing. We provide functional validation and characterization of many gene parts in several Chlamydomonas strains. This kit is available to the community, to allow Chlamydomonas to become the next chassis for sustainable synthetic biology approaches.

RESULTS

Standard and Content of the Chlamydomonas MoClo Kit. Standardization is the key to efficient building. The Chlamydomonas MoClo kit adopts the syntax proposed by the plant synthetic biology community including the OpenPlant Consortium[30] (Figure 1). This syntax is defined for level 0 plasmids containing standard gene parts (promoters, coding sequences, untranslated regions, etc.) and assigns strict fusion sites for 10 cloning positions. In a single step, standardized parts can be assembled into modules (Transcriptional Unit, TU, level 1) and modules into devices (multigenic construct, level M or 2) according to the original MoClo syntax[22] (Supplementary Figure 1). Our Chlamydomonas MoClo toolkit is composed of a set of 119 parts representing

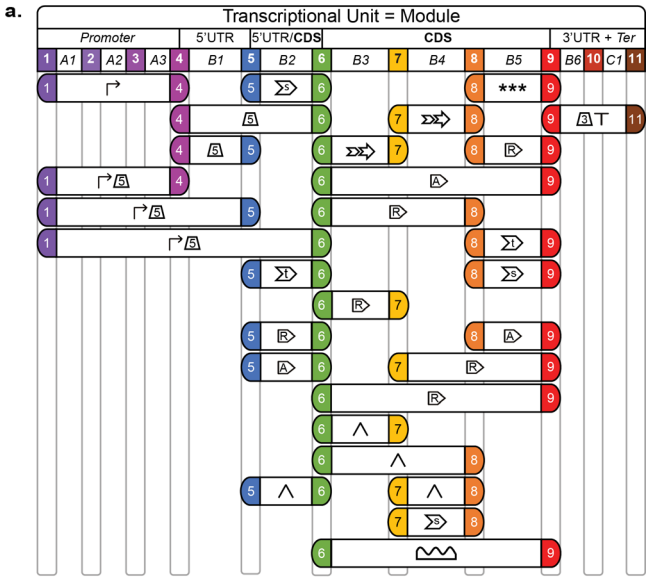

b.

Types of part (*non transcribed*; **translated**)	SBOL	Parts	Unique parts
Promoters		7	7
Promoters + 5'UTR		15	7
5'UTR		12	6
Introns		4	1
Signal and Targeting peptides		11	9
Immuno and purification tags		15	8
Reporter genes		34	12
Antibiotic Resistance genes		8	5
3'UTR / *Terminators*		6	6
2A peptide		2	1
amiR		4	4
Multi-Stop	***	1	1
Total		119	67

Figure 1. Overview of the Chlamydomonas MoClo toolkit. (a) Type and position of parts used following the Plant MoClo Syntax.[30] Symbols correspond to the SBOL2.0 visual[69] representation described in part b. Each of the 11 fusion sites defining a part position is represented with a color and a number. Positions presented are representative of the whole set of each part type. Parts in italicized letters are nontranscribed, parts in regular letters are transcribed, and parts in bold letters are transcribed and translated. (b) Table summarizing unique and total gene parts available. The SBOL2.0 symbols are indicated for each type. When the SBOL2.0 standard was not existing for a part type, the symbol proposed in a previous work[28] was used, or defined here.

67 unique genetic elements available at different positions within the standard, thereby providing maximum modularity to designers (Figure 1, Figure 2). The kit recapitulates most of the standard genetic elements previously developed for Chlamydomonas which we "domesticated" by removing *Bpi*I and *Bsa*I restriction sites (the two enzymes used by the MoClo strategy,[22] Supplementary Figure 1) from their sequences by DNA synthesis or PCR-based mutagenesis. The available gene parts encompass seven promoters coupled or not to their original 5′UTR, the corresponding 5′UTR, and the *CrTHI4* riboswitch, eight immunological or purification tags in positions leading to N- or C-terminal translational fusions, nine signal and targeting peptides, 12 reporters, five antibiotic resistance genes, the foot and mouth virus (FMDV) 2A peptide which allows expression of two or more proteins from a single transcriptional unit,[17,31,32] two micro RNA (miRNA) backbones and associated controls, and six 3′UTR-terminators

DOI: 10.1021/acssynbio.8b00251
ACS Synth. Biol. 2018, 7, 2074−2086

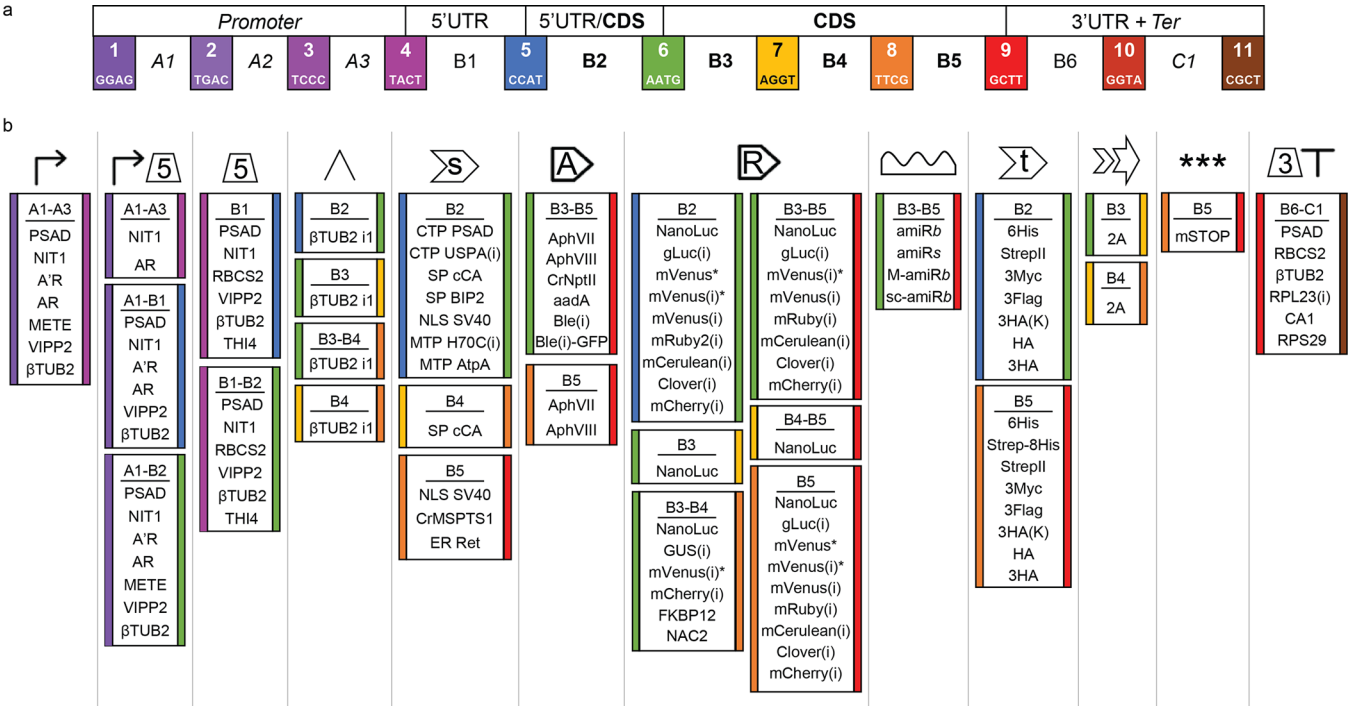

Figure 2. List of parts in function of their type and assembly position. (a) Plant MoClo syntax[30] indicating the color code for fusion sites used in this figure. (b) All parts in the Chlamydomonas MoClo kit are classified primarily by their function, indicated by SBOL2.0 visual code[69] as in Figure 1 (from left to right: promoters, promoter+5'UTR, 5'UTR, introns, antibiotic resistance genes, reporter genes, artificial microRNA, immunological and purification tags, 2A peptide, and 3'UTR+terminators). Colored stripes on the left and right sides of each box represent the fusion sites in 5' and 3' of the position, respectively, and follow the color code on top. AR and A'R stand for HSP70A/RBCS2 and HSP70A467/RBCS2, respectively.[36] A star (*) indicates that the part contains extra restriction sites as in pOpt vectors[68] while the same part unmarked does not. An (i) indicates the presence of an intron within the part (cf. Supplementary Table 2). For amiRNA (amiR) backbones, *b* and *s* mean that *Bpi*I and *Spe*I site are within the backbone for amiR cloning, respectively, while M and sc mean that the target amiR sequence for MAA7 and the control scrambled sequence were introduced into the miR1157 backbone, respectively (cf. Figure 4). mSTOP stands for multi-STOP.

(Figure 1b, Figure 2, and Supplementary Table 1). All sequences and plasmids are available through the public Addgene repository (http://www.addgene.org/).

Constitutive Promoters and Reporter Genes. Five antibiotic resistance genes are used as selectable markers for Chlamydomonas but also can function as reporter genes.[33,34] We assembled three modules that allow control of the expression of the *aadA* gene, conferring spectinomycin resistance, by three constitutive promoters: P_{PSAD} and $P_{\beta TUB2}$ with or without the first intron of *βTUB2* (pCM1-1 to 3, Supplementary Table 3). The transformation efficiency of the three modules in UVM4[35] cells was estimated by counting spectinomycin resistant colonies and showed resistance frequencies within the same range (Figure 3a). The presence of the first *βTUB2* intron significantly increased the transformation efficiency as previously observed with the presence of *RBCS2* introns in the *ble* marker.[33,36,37] Alternative reporters are bioluminescent proteins, which allow more sensitive and quantitative analysis of gene expression. The kit contains *Gaussia princeps* luciferase, the brightest luciferase established in Chlamydomonas,[38] as well as the redesigned Nanoluciferase (NanoLuc) which provides a stable and strong luminescence signal.[39] Chlamydomonas NanoLuc was specifically developed for our MoClo kit through recoding to match the codon bias of Chlamydomonas, and cloned at six different positions within the standard. This new part was first tested with the most widely used promoter/terminator combination (P_{AR} promoter/T_{RBCS2} terminator) for strong constitutive expression in Chlamydomonas. The corresponding module (pCM1-04) was assembled with another module conferring paromomycin resistance (Supplementary Figure 2) into a device (pCMM-1) that was introduced into the genome of the D66 strain (CC-4425, Figure 3b). Among paromomycin resistant colonies, 34.8% ± 8.3 (N = 48, mean ± SEM) were luminescent. The signal was variable between clones due to genomic position effects[40,41] but was linear from 50 to 5 × 10^5 cells (Figure 3b and Supplementary Figure 2). By contrast, nonexpressing transformants (resistant to paromomycin only) or the D66 recipient strain displayed only a faint signal, 3 orders of magnitude lower, and saturating swiftly (Figure 3b, inset). The modularity of the MoClo strategy allows rapid assessment of combinations of multiple parts. For example, we assembled four modules for which NanoLuc expression is controlled by all possible combinations of the two most common constitutive promoters (P_{AR} and P_{PSAD}) and terminators (T_{RBCS2} and T_{PSAD}) (Figure 3b, pCM1-4 to 7, Supplementary Table 3). Each module was assembled with the paromomycin resistance module (pCMM-1 to 4, Supplementary Table 4) and introduced into the Chlamydomonas genome. Bioluminescence levels were averaged over hundreds of transformants to account for the genome position effect.[40,41] The strengths of the two promoters were found to be comparable, while T_{PSAD} appeared to confer robust expression from both promoters, 10-fold higher than T_{RBCS2} (Figure 3c). In a distinct context (strain, reporter sequence, culture conditions, etc.), the same genetic element may perform differently.[31,35] Such context sensitivity can be overcome by taking advantage of the modularity of the Chlamydomonas MoClo kit, which

DOI: 10.1021/acssynbio.8b00251
ACS Synth. Biol. 2018, 7, 2074−2086

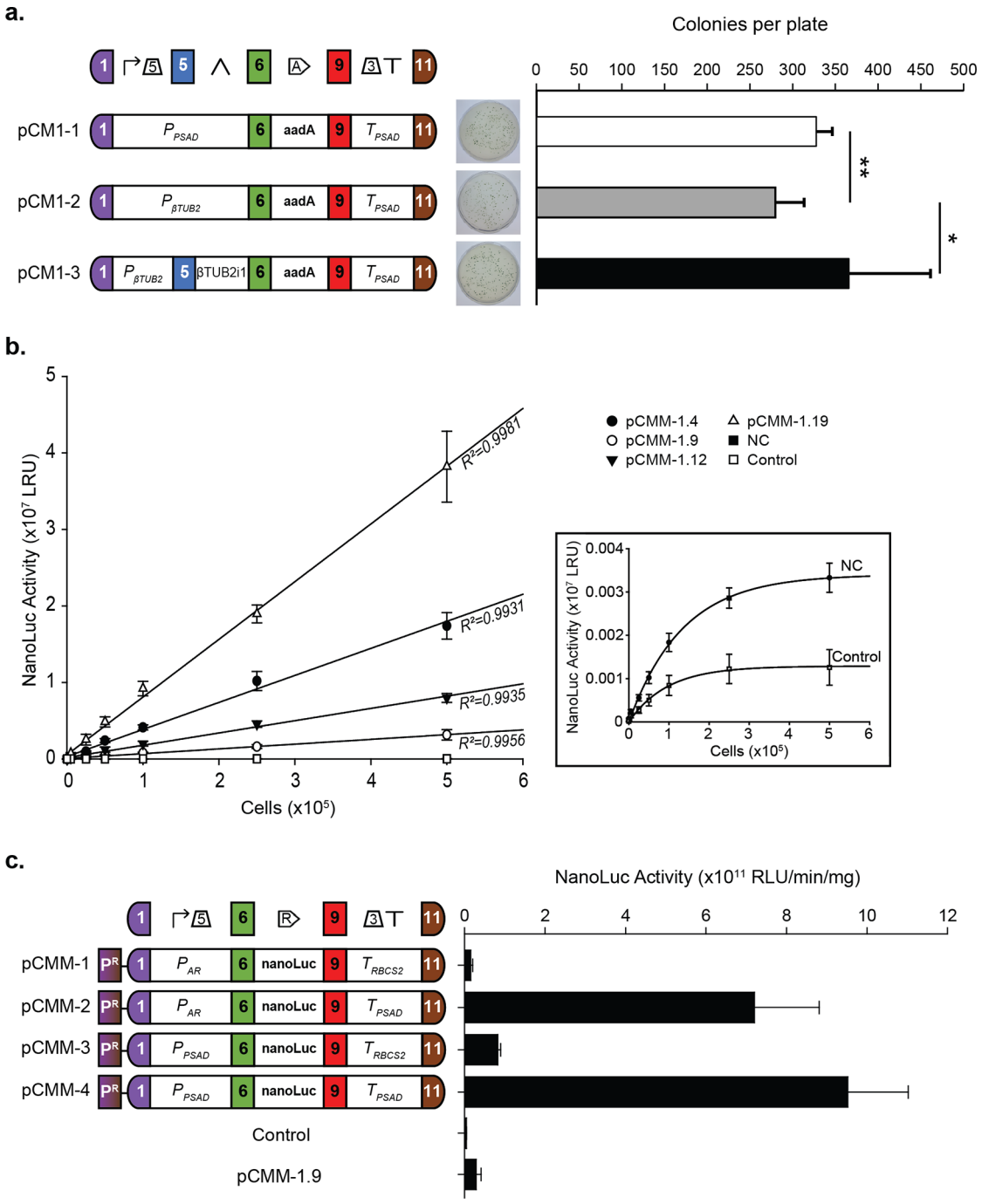

Figure 3. Constitutive promoters and reporter genes. (a) Average number of spectinomycin resistant colonies after transformation of UVM4 cells (mean ± SD, $N = 11$) for the three modules (pCM1-3, where pCM stands for plasmid Chlamydomonas MoClo). Representative transformation plates are shown. (b) Linearity of NanoLuc activity as a function of cell number. NanoLuc activity for four independent clones transformed with the pCMM-1 device (pCMM-1.X), one nonexpressing clone (NC) and the recipient strain (CC-4425 noted as control) are presented ($N = 3$, mean ± SEM). Linear regression and correlation coefficient (R^2) are shown. The NC and control are shown in the inset on a different scale. (c) Average NanoLuc activity of D66 (CC-4425) cells transformed with four devices (pCMM-1 to 4) harboring promoter/terminator combinations to drive NanoLuc expression coupled to a paromomycin resistance module (represented as P^R, left, Supplementary Figure 2). Luminescence levels are represented as mean ± SEM (average of a total of more than 400 clones from three biological replicates). The negative and positive controls are the recipient strain and the pCMM-1.9 strain (shown in panel b), respectively. (a,c) *$p < 0.05$; **$p < 0.01$ assessed by Student's t test, SBOL2.0[69] visual of module designs are shown above the devices.

allows for the rapid characterization of all possible parts combinations. These results also confirmed the performance of the Chlamydomonas NanoLuc reporter and its employability for detailed understanding and characterization of genetic circuits especially if coupled with automated cell-sorting microfluidic devices.[42]

Control of Gene Expression. To build genetic circuits, the fine-tuning of gene expression is a prerequisite. Multiple parts enabling controlled gene expression have therefore been

DOI: 10.1021/acssynbio.8b00251
ACS Synth. Biol. 2018, 7, 2074−2086

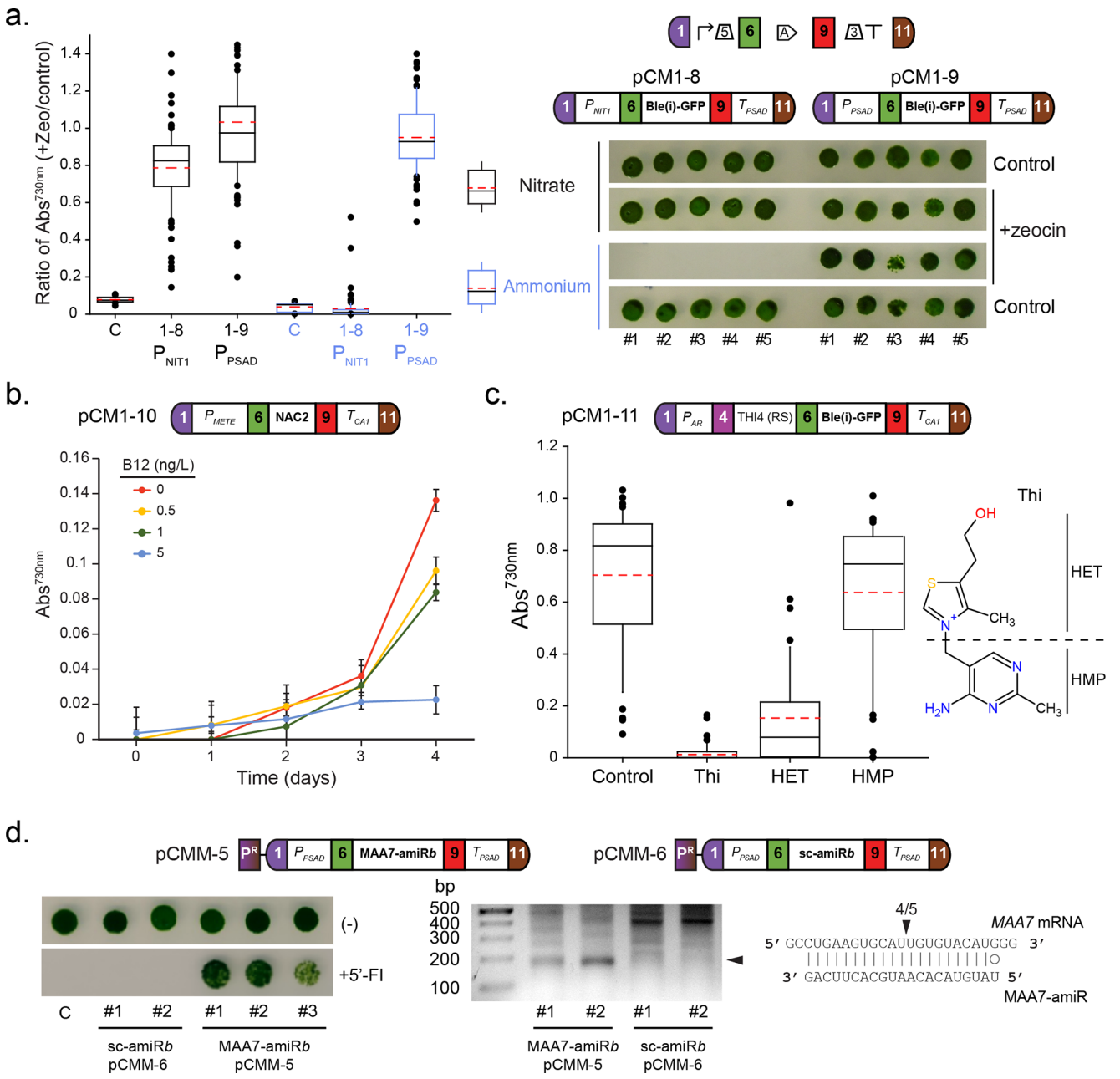

Figure 4. Control of gene expression. (a) Control of gene expression by the nitrogen source. Zeocin resistant colonies (conferred by *Ble(i)-GFP*) selected after transformation of CC-1690 cells with each of the two represented modules ("1-8" for pCM1-8 and "1-9" for pCM1-9) were grown in TAP-nitrogen ± zeocin (15 μg/mL) supplemented with either 7.5 mM $(NH_4)Cl$ (ammonium, blue) or 4 mM KNO_3 (nitrate, black) and their growth was followed (absorbance at 730 nm). The plot shows the ratio between the growth in the presence and absence of zeocin (C is the nontransformed CC-1690 strain). The right panel shows cells grown in similar conditions but on solid media. Results presented (N = 16 for control CC-1690 and N = 86 for each other conditions) correspond to one out of three independent transformations (for the other two, see Supplementary Figure 3). (b) Control of gene expression by vitamin B_{12}. Conditional complementation of *nac2-26* cells with the pCM1-10 module expressing NAC2 under P_{METE} control. Complemented strains were selected for photoautotrophic growth on solid minimal medium and the cells were grown in liquid minimal medium supplemented with the indicated amount of vitamin B_{12}. Data are mean ± SD (N = 3). (c) Control of gene expression by vitamin B_1. Average growth (absorbance at 730 nm after 7 days of growth, N = 40) of UVM4 cells transformed with the pCM1-11 module designed to express constitutively *Ble(i)-GFP* transcripts containing the *THI4* riboswitch in the 5′UTR. After culture in TAP, the cells were transferred to TAP+zeocin (10 μg/mL) supplemented with 10 μM thiamine (Thi), 10 μM 4-methyl-5-(2-hydroxyethyl) thiazole (HET), or 10 μM 4-amino-5-hydroxymethyl-2-methylpyrimidine (HMP) or not (control). The chemical structure of Thi is represented on the right and the HET and HMP moieties are indicated (see also Supplementary Figure 3). (d) Targeted gene knockdown with artificial miRNA. Paromomycin resistant cells selected after transformation of CC-1690 cells by each of the two represented devices (pCMM-5 and pCMM-6), carrying an amiRNA cloned with *Bpi*I and directed against *MAA7* (MAA7-amiR*b*) or a random sequence ("scrambled": sc-amiR*b*), were grown in the absence (denoted (−)) or presence of 5′-fluoroindole (+5′-FI) (left panel). C indicates nontransformed cells. Clones resistant to 5′FI were analyzed by a modified 5′-RACE assay. A specific 173 bp PCR band (black arrowhead) was amplified only from the 5′-FI resistant transformants and not from ones expressing the amiRNA with scrambled sequence (middle panel and Supplementary Figure 3). Sequencing revealed that the most frequent cleavage occurred at positions opposed to positions 10 and 11 of the amiRNA (right panel, black arrowhead). P^R represents the paromomycin resistance module

DOI: 10.1021/acssynbio.8b00251
ACS Synth. Biol. 2018, 7, 2074−2086

Figure 4. continued

(pCM1-27, Supplementary Figure 2a). (a,c) The box and whisker plots show the 10th (lower whisker), 25th (base of box), 75th (top of box), and 90th (top whisker) percentiles. The line within the box is the median, the dashed red line is the mean. Outliers are plotted as individual data points.

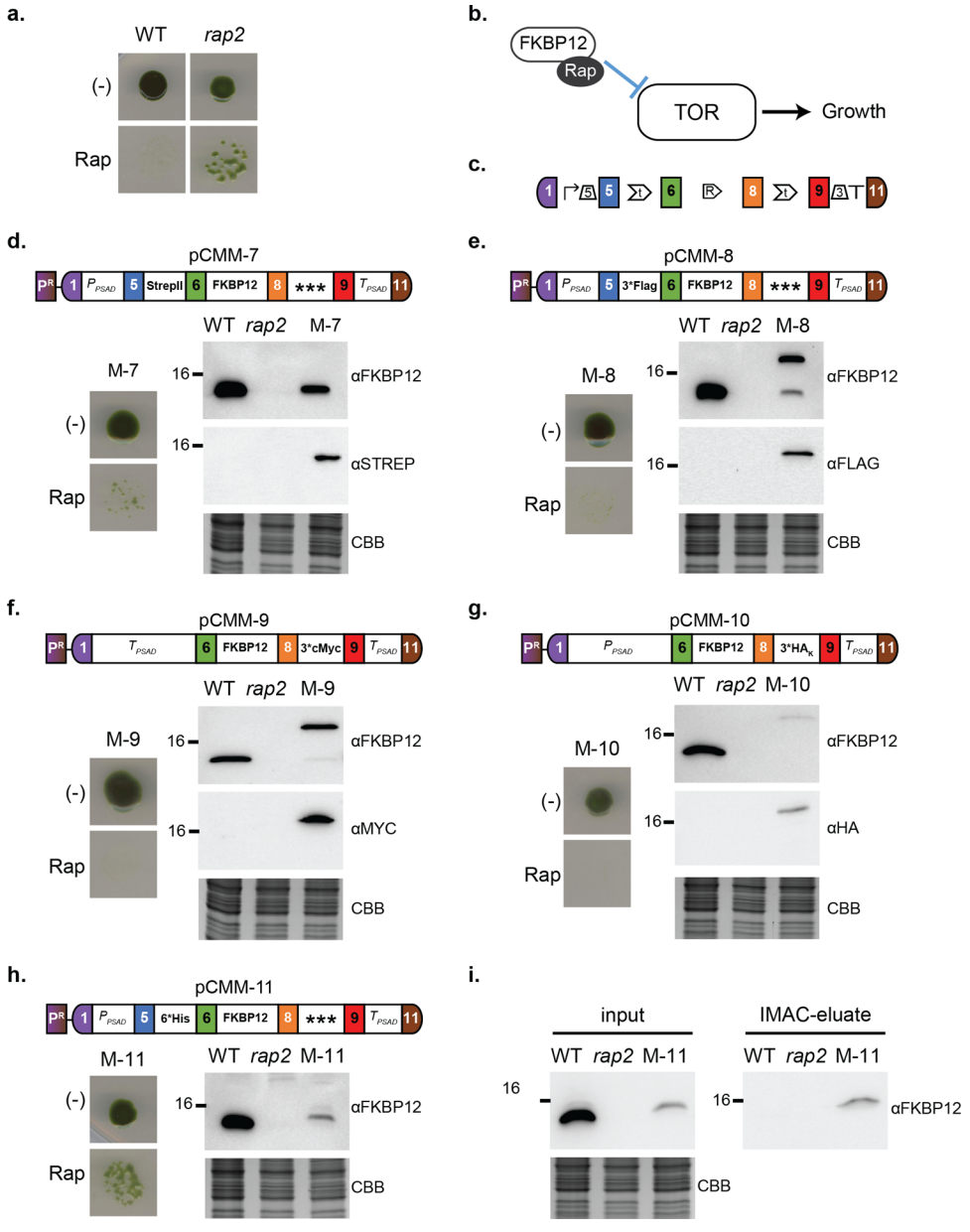

Figure 5. Design, build, and test of five fusion tags. (a) Phenotype of recipient (WT) and Δ*FKBP12* (*rap2*) strains in the presence (Rap) or absence (−) of 1 μM rapamycin. (b) Molecular mechanism underlying the *rap2* phenotype. Target Of Rapamycin (TOR) is inhibited by rapamycin only in the presence of FKBP12 (mutated in *rap2*). Upon formation of the tripartite TOR/FKBP12/rapamycin complex, TOR is inhibited and growth is arrested.[52] (c) SBOL2.0 visual[69] of module designs for functional complementation of *rap2*. (d−h) Phenotype in the presence (Rap) or absence (−) of 1 μM rapamycin and detection of tagged proteins in soluble extracts by immunoblotting with antibodies against either FKBP12 (αFKBP12) or the appropriate tag (indicated within each panel). Each device is indicated in the upper part of the panel. CBB: Coomassie Brilliant Blue staining of a duplicate gel loaded with the same samples and shown as loading control. (i) Purification through ion-metal affinity chromatography (IMAC) of 6His-FKBP12 expressed from the same device as in panel h. P^R represents the paromomycin resistance module (pCM1-27, Supplementary Figure 2a). *rap2* cells transformed with pCMM-X are indicated as M-X in each panel. Data are representative of three biological replicates.

implemented. The activity of the P_{NIT1} promoter can be controlled by switching the nitrogen source since it is strongly repressed by ammonium and highly induced on nitrate.[34,43,44] A module where P_{NIT1} controls expression of the *Ble-GFP* gene (pCM1-8) conferred strong zeocin resistance in the CC-1690 strain but only when ammonium was replaced by nitrate as the nitrogen source. By contrast, the P_{PSAD} promoter (pCM1-9) conferred strong antibiotic resistance on both nitrogen sources (Figure 4a and Supplementary Figure 3a-c). The vitamin B_{12}-repressible promoter P_{METE}[45] allowed conditional functional

DOI: 10.1021/acssynbio.8b00251
ACS Synth. Biol. 2018, 7, 2074−2086

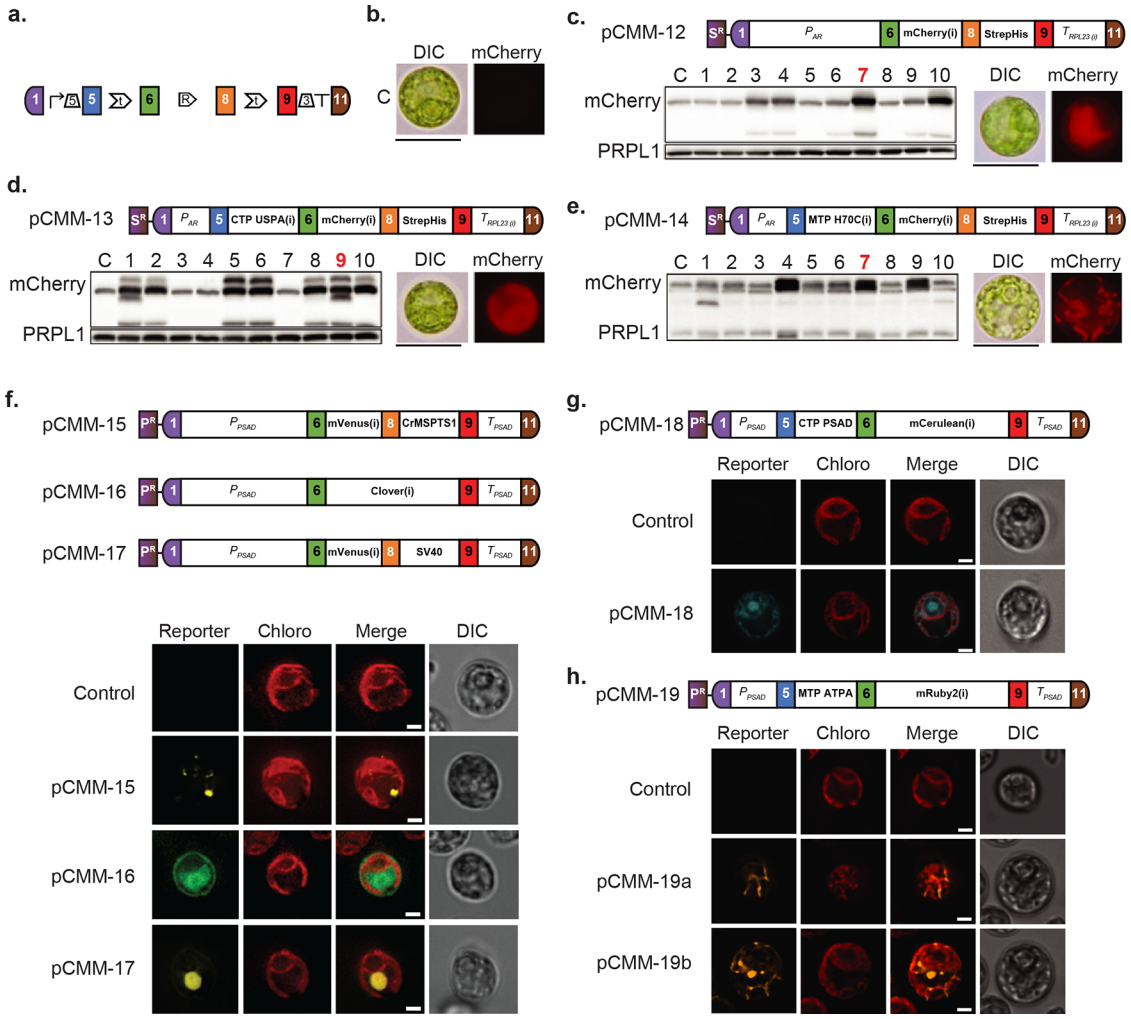

Figure 6. Targeting reporter genes to different subcellular compartments. (a) SBOL2.0[69] visual syntax for modules used. (b) Visible light ("DIC") and fluorescence signal ("mCherry") of the UVM4 recipient strain used as control ("C") for panels c–e. (c-e) mCherry targeting to the (c) cytosol with no transit peptide, (d) chloroplast with CTP USPA (Chloroplast Transit Peptide of Universal Stress Protein A) or (e) mitochondria with MTP H70C (Mitochondrial Transit Peptide of HSP70C) in UVM4 cells transformed with the indicated devices (pCMM-12 to 14). In each panel, an anti-mCherry immunoblot analysis of transformants is shown. Note that the anti-mCherry antibody cross-reacts with a protein of similar size present in control cells (C). An anti-PRPL1 immunoblot is shown as loading control. The transformant strain number indicated in red corresponds to the images (bars are 10 μm) presented on the right. (f–h) Fluorescent marking of (f) microbodies with mVenus-CrMSPTS1 (Malate Synthase PTS1-like sequence), cytosol with Clover or the nucleus with mVenus-SV40 (Simian Virus 40 nuclear localization signal), (g) the chloroplast with CTP PSAD-mCerulean (Chloroplast Transit Peptide of PSAD), (h) mitochondria with MTP ATPA-mRuby2 (Mitochondrial Transit Peptide of ATPA) after transformation of UVM4 cells with the indicated devices (pCMM-15 to 19). Images of representative transformants are grouped with the corresponding control image (recipient strain) according to the filter used. pCMM-19a and pCMM-19b show two images taken on different *z*-axis on the same cell. "Chloro" refers to chlorophyll autofluorescence. The scale bars represent 2 μm. S^R and P^R represent, respectively, modules conferring resistance to spectinomycin (S^R = pCM1-1, Figure 3a and Supplementary Figure 2a) and paromomycin (P^R = pCM1-27, Supplementary Figure 2a).

complementation of the photosynthetic mutant *nac2-26* (CC-4421), which lacks photosystem II due to the absence of the TPR-like protein NAC2 required for stability of the *psbD* mRNA encoding the D2 reaction center protein.[46] *nac2-26* mutant cells engineered with a module harboring the *NAC2* coding sequence under the control of the P_{METE} promoter (pCM1-10) could grow photoautotrophically in the absence of vitamin B_{12}, but growth was compromised by increasing its concentration by amounts as low as 5 ng/L (Figure 4b).

Regulation of gene expression can also be controlled by vitamin B_1 (thiamine) at the level of the transcript through riboswitches.[47,48] Binding of thiamine pyrophosphate to the *THI4* riboswitch (RS) results in alternative splicing and retention of an 81 bp upstream open reading frame, ultimately interfering with translation.[47,48] The RS also responds when cells are grown in the presence of the thiamine biosynthetic intermediate 4-methyl-5-(2-hydroxyethyl) thiazole (HET), but not with 4-amino-5-hydroxymethyl-2-methylpyrimidine (HMP).[47] A module combining P_{AR} and *THI4 (RS)* to drive expression of the *ble-GFP* gene (pCM1-11) conferred conditional zeocin sensitivity in the UVM4 strain.[35] Resistance was compromised by thiamine or HET but not HMP (Figure 4c and Supplementary Figure 3d), thereby demonstrating the efficient repression of the transgene through the *THI4* riboswitch.

Finally, to allow targeted repression of gene expression, a microRNA precursor sequence derived from the pre-miR1157 and used for the generation of artificial miRNAs (amiRNA)[49]

DOI: 10.1021/acssynbio.8b00251
ACS Synth. Biol. 2018, 7, 2074–2086

was redesigned for compatibility with the Golden Gate cloning method. To demonstrate its effectiveness in driving gene repression, a specific amiRNA sequence directed against the *MAA7* gene, whose repression provides resistance to 5′-fluoroindole (5′-FI),[50] was inserted into the microRNA precursor. A control random sequence ("scrambled") amiRNA was inserted into the same backbone. These parts were placed under the control of P_{PSAD} and T_{PSAD} (pCM1-12 and 13) and assembled with a paromomycin resistance module (pCM1-27). The same amiRNA sequences were introduced into the previously established pChlamiRNA3 vector[49] as controls. After transformation of the CC-1690 strain, 36% of paromomycin-resistant cells displayed resistance to 5′-FI with the device targeting *MAA7* (pCMM-5) but not with the scrambled amiRNA (pCMM-6) (Figure 4d and Supplementary Figure 3f). A modified 5′ rapid amplification of cDNA ends (5′-RACE) assay revealed that the *MAA7* transcript was most frequently cleaved at a site corresponding to positions 10 and 11 of the amiRNA, as expected for a specific action of the miRNA (Figure 4d). The properties of controllable parts can also be combined as shown for P_{NIT1} control of amiRNA-dependent gene repression.[34] An amiRNA strategy recently proved useful for concerted metabolic engineering of a biodiesel precursor in Chlamydomonas.[8] The versatility of the MoClo kit opens new possibilities for sophisticated metabolic engineering strategies, for example, the specific downregulation of up to six target genes with one level M assembly.

Multiple Fusion Tags for Detection and Purification of Gene Products. Protein fusion tags are indispensable tools used to improve protein expression yields, enable protein purification, and accelerate the characterization of protein structure and function.[51] Our MoClo kit includes multiple epitope and affinity tags known to be functional in Chlamydomonas. The modularity of the MoClo assembly allows rapid assessment of the best tagging strategy through a rapid design/build/test/learn cycle. We took advantage of the well characterized *rap2* mutant (Δ*FKBP12*), which is insensitive to rapamycin,[52] to test the functionality of five tags (Figure 5a,b). We designed and built 5 devices allowing strong constitutive expression of N- or C-terminal tagged FKBP12 coupled to a paromomycin module (pCMM-7 to 11, Figure 5c–h and Supplementary Table 4). The engineered strains were selected on paromomycin and the functionality of the fusion protein was tested by assessing sensitivity to rapamycin. Protein extracts were probed by immunoblotting using FKBP12-specific and tag-specific antibodies (Figure 5d–h). All tags allowed detection (Figure 5d–h) or purification (Figure 5i) of FKBP12 even though some were not functional for restoring rapamycin sensitivity. The test revealed that pCMM-9 outperforms other devices since it provides a WT-like phenotype and expression level coupled to a strong and specific Myc signal with no significant processing of the protein. These results demonstrate the importance of the modularity provided by the Chlamydomonas MoClo toolkit for designing optimal fusion proteins.

Visualization and Targeting of Proteins in Living Cells. Fluorescent protein tags allow the temporal and spatial monitoring of dynamic expression patterns at cellular and subcellular scales.[53] Natural and synthetic metabolic pathways can be optimized through spatial organization since cell compartments offer many advantages, such as isolation of metabolic reactions and generation of concentration gradients.[14] In a eukaryotic chassis like Chlamydomonas, organelles such as microbodies, mitochondria, and chloroplasts can be engineered to implement or improve metabolic pathways.[15] The Chlamydomonas MoClo kit includes 11 targeting and signal peptides that allow the targeting of fusion proteins to mitochondria, chloroplast, nucleus, secretory pathway, ER, and peroxisome-like microbodies. The functionality of the targeting and signal peptides and of the five fluorescent proteins (mVenus, yellow; mCherry, red; mRuby2, red; Clover, green; mCerulean3, cyan) included in the toolkit was tested. Eight modules (pCM1-19 to 26, Supplementary Table 3) combining diverse fluorescent proteins and targeting sequences were assembled into devices with an antibiotic resistance module (pCMM-12 to 19). All devices were found to behave as expected and provided the expected fluorescent signal in the targeted compartment (Figure 6). The fluorescent and targeting parts of the Chlamydomonas MoClo toolkit, most of which have been validated here, enable engineering in the third dimension[14] that is, isolation and organization in multiple cellular compartments, and offer new tools for biological design/build/test cycles.

DISCUSSION

The Chlamydomonas MoClo toolkit presented here provides more than 100 domesticated gene parts to allow advanced synthetic biology in microalgae. Numerous parts of multiple types have been characterized and validated in different genetic backgrounds[10] and culture conditions, and can be readily used for biological design without further development. With the efficiency and modularity of the MoClo strategy, molecular cloning is no longer a limiting step for engineering Chlamydomonas cells. Indeed, from design to building, a complex device of up to six different genes/modules can be obtained within a week using the standardized parts provided in our kit. The modularity will also enable combinatorial assembly by shuffling part libraries[54] and determine *a posteriori* which combination is the most relevant. The development of gene-editing technologies in Chlamydomonas, including Zinc-finger nucleases[55,56] and several CRISPR-Cas9 approaches,[55,57−59] together with the development of high-throughput microfluidics[42] are beginning to gather pace. Coupling these resources to our standardized MoClo toolkit will facilitate the use of Chlamydomonas as the photosynthetic chassis for innovative synthetic biology approaches aimed at fundamental and biotechnological applications. We expect that the creativity of designers, released from the time constraints associated with classical cloning strategies, will allow rapid expansion of the standard gene parts, modules, and devices through open distribution, notably using the Addgene repository. We invite the community to openly share their parts through Addgene and/or our consortium (contact M. Schroda). The development of the Chlamydomonas MoClo toolkit constitutes a complete step-change in the fields of microalgal biology and biotechnology. The parts developed for the MoClo toolkit may also be employed in other microalgal species since the orthogonality of several Chlamydomonas transcriptional units has been demonstrated in multiple hosts, including the industrially relevant species *Chlorella ellipsoidea*, *Nannochloropsis sp.* and *Dunaliella salina*.[60] Synthetic approaches will allow engineering of microalgae in a predictable and efficient manner and thereby offer great potential to couple environmental protection, energy transition, and bioeconomic growth.[4]

DOI: 10.1021/acssynbio.8b00251
ACS Synth. Biol. 2018, 7, 2074−2086

METHODS

All chemicals were obtained from Sigma-Aldrich, unless otherwise specified.

***Escherichia coli* and *Chlamydomonas reinhardtii* Strains, Transformation, and Growth Conditions.** Bacterial growth was performed at 37 °C in LB broth supplemented with agar (20% m/V), spectinomycin (50 μg/mL), ampicillin or carbenicillin (50 or 100 μg/mL, respectively) and X-gal (40 μg/mL) when required. Chemically competent *E. coli* DH10β (New England Biolabs) were used for transformation (by heat shock following the manufacturer's instructions) and maintenance of plasmids. All plasmids of the kit were maintained and amplified in TOP10 *E. coli* strain prior to submission to Addgene.

C. reinhardtii strains,[35,46,52,61,62] culture and transformation conditions are recapitulated in Supplementary Table 5. They were grown in Tris-acetate-phosphate (TAP) medium[63] supplemented with agar (1.6% m/V), spectinomycin (100 μg/mL), paromomycin (15 μg/mL), zeocin (ThermoFisher Scientific, 10 to 15 μg/mL), 5-fluoroindole (20 μM) or rapamycin (LC Laboratories, 1 μM) when required. For *NIT1* promoter characterization (Figure 4a), a modified TAP medium lacking nitrogen source (TAP-N) was used instead, and was supplemented with 4 mM KNO_3 (nitrate) or 7.5 mM NH_4Cl (ammonium). For NAC2 autotrophy test (Figure 4b), cells were grown in minimal media (HSM) for selection of complemented strains. The responsiveness to B12 was assessed on plate and then in liquid. Cells were grown for 15 days in HSM until 1−5 × 10^7 cells/mL concentration was reached prior to inoculation in a 96-well plate at a concentration of 10^5 cells/mL in 200 μL of HSM. For response assays (Figure 4c) thiamine (Melford Laboratories Ltd.), 4-methyl-5-(2-hydroxyethyl) thiazole (HET) and 4-amino-5-hydroxymethyl-2-methylpyrimidine (HMP, Fluorochem UK) were added to TAP media at a final concentration of 10 μM.

For transformation by electroporation (see Supplementary Table 5), a TAP culture of (1−5) × 10^6 cells/mL was concentrated 100 times in TAP complemented with 60 mM sucrose or the MAX Efficiency Transformation reagent for Algae (ThermoFisher scientific) and 25−250 μL were incubated with 80−300 ng of DNA for 10−30 min on ice in a 0.4 cm gapped cuvette (BioRad) prior to electroporation (BioRad Gene Pulser Xcell). The cells were then left to recover in TAP complemented with 40−60 mM sucrose for 16 h under appropriate light and shaking conditions (typically 50 μmol photon m^{-2} s^{-1} at 100 rpm) prior to plating on TAP-agar plates with adapted antibiotics. Transformation by glass-beads method followed previously published protocols.[7,64] Briefly, after growth in TAP until 5 × 10^6 cells/mL, cells were concentrated 30 times and 5 × 10^7 cells were mixed with DNA using glass beads. After 2-fold dilution with TAP, 2.5 × 10^7 cells were spread onto TAP agar plates containing 100 μg mL^{-1} spectinomycin. Plates were incubated for 16 h in the dark prior to light exposition (30 μmol photon·m^{-2}·s^{-1}). When colony counting was performed (Figure 3a), it was 8 days after the beginning of light. In both cases, the transformation protocol leads to insertion of a linear DNA in a random location within the nuclear genome.

Design. All *in silico* sequence designs and analysis were performed with Serial Cloner, Benchling, SnapGene, ApE or Genome Compiler. For exogenous parts, reverse translation was performed with Serial Cloner using *C. reinhardtii* nuclear genome codon frequency (http://www.kazusa.or.jp/codon/cgi-bin/showcodon.cgi?species=3055).

amiRNAs can be generated using DNA parts pCM0-068 and pCM0-069. Both are derived from the endogenous pre-miR1157,[65] but differ in the way in which the amiRNA specific sequence is introduced. pCM0-069/pCMM-20 is analogous to pChlamyRNA3,[65] and a dsDNA fragment containing the amiRNA/loop/amiRNA* sequence is introduced into a *Spe*I site inside the miRNA precursor sequence. pCM0-068 presents two divergently oriented *Bpi*I sites, allowing the cloning of the dsDNA fragment by Golden Gate. In this last case, the dsDNA fragment is formed by the annealing of two oligos with the following sequence: (1) sense oligo (5′ AGTA-(MIRNA*-SEQ)-TCTCGCTGATCGGCACCATGGGGGTGG-TGGTGATCAGCGCTA-(MIRNA SEQ)-T 3′), (2) antisense oligo (5′CAGT-A-(rev com MIRNA SEQ)- TAGCGC-TGATCACCACCACCCCCATGGTGCCGATCA-GCGAGA-(rev com MIRNA*SEQ) 3′). There are online tools that help with the design of the amiRNA sequence (http://wmd3.weigelworld.org/cgi-bin/webapp.cgi).

Parts Repository. All sequences listed in Supplementary Table 2 were deposited in Addgene. Physical distribution of the DNA is performed through Addgene. We invite the community to share their future parts through Addgene and/or with our consortium (contact M. Schroda) which will make them available to the community.

Parts Cloning. All PCR reactions were performed using the Phusion DNA polymerase, KOD Xtreme Hot Start DNA polymerase (Merck), or Q5 DNA polymerase purchased from New England Biolabs (NEB) following the manufacturer's instructions adapted to GC-rich DNA, typically duration of hybridization and polymerization was doubled and/or GC enhancer solution was used. Molecular biology kits were purchased from Macherey-Nagel, peqLab, NEB or QIAgen (gel extraction and miniprep kits). Primers were produced by Eurofins Genomics or Sigma-Aldrich, while synthesized parts were obtained from Genecust, DC Biosciences, IDTDNA or Sigma-Aldrich.

MoClo Assembly Conditions. All Restriction/ligation reactions were performed using *Bbs*I or *Bbs*I-HF (*Bpi*I is an isoschizomer) or *Bsa*I-HF (NEB or ThermoFisher) together with T4 ligase (NEB) in a medium containing the NEB CutSmart buffer and 1 mM ATP (with stock of 10 mM solubilized in 0.1 M Tris-HCl, pH 7.9). Typical ratio between destination plasmid (100 fmol) and entry plasmid/parts was 1:2. To facilitate handling of the kit for end-users, we provide detailed protocols and reaction mix calculators for each type of assembly: level 0 for parts (Supplementary Table 6), level 1 for modules (Supplementary Table 7) and level M for devices (Supplementary Table 8).

Quality Control of Generated DNAs. All plasmids were controlled by differential restriction. In addition, all level 0 plasmids were sequenced with specific primers. Sequencing was performed by Eurofins Genomics, Source BioSciences UK, Seqlab, Macrogen, Microsynth, GATC Biotech or Core Facility (CeBiTec, Bielefeld University).

NanoLuc Activity Determination. Reagents were purchased from Promega (ref N1110) and activity was determined as previously described.[39] For screening, *C. reinhardtii* colonies were transferred into a 96-well plate containing 100 μL of TAP in each well. After gentle resuspension, 50 μL was transferred into a solid white 96-well plate to which 50 μL of Nano-Glo substrate diluted in the

DOI: 10.1021/acssynbio.8b00251
ACS Synth. Biol. 2018, 7, 2074−2086

provided buffer (2% V/V) was added and gently mixed by pipetting. Luminescence was measured at 460 nm with a CLARIOstar plate reader (BMG Labtech). For promoter/terminator combination assessment experiment (Figure 3c), all *C. reinhardtii* colonies from a transformation event were pooled and resuspended in TE buffer (50 mM Tris-HCl pH 7.9, 1 mM EDTA) complemented with antiprotease (1 tablet per 50 mL, Sigma-Aldrich: S8830). The cells were lysed by vortexing 10 s twice in the presence of glass beads (about 1:5 ratio beads/cells V/V) prior to two centrifugations (20000*g* for 10 min at 4 °C) to clarify the supernatant. The protein concentration was then determined using Bradford reagent with a Bovine Serum Albumin standard curve and the concentration was standardized to 0.5 g/L. The activity was determined in a 96-well plate in a final volume of 50 μL (1:1 with nano-Glo resuspended in provided lysis buffer) per well. NanoLuc activity was determined on six different increasing protein quantities (0.1 to 2.5 μg) for each assay, allowing to assess the linearity of the signal.

Absorbance Measurement of Cultures Growing in Microtiter Plates. Growth in microtiter plates was determined by measuring the optical density of each well at 730 nm. Microtiter plates containing 180−200 μL culture were incubated under constant light (125 μmol photon·m^{-2}·s^{-1}) at 25 °C and 40 rpm orbital shaking. For density determination, cultures were resuspended by pipetting and 100 μL of cell suspension was transferred to a new microtiter plate containing 50 μL TAP 0.03% Tween-20. The optical density of each well was determined at 730 nm in a CLARIOstar plate reader (BMG Labtech). Plates were shaken for 6−10 s at 600 rpm before measurement.

RNA Extraction and miRNA-Mediated Cleavage Mapping. RNA isolation was carried out as previously described[49] (a detailed protocol can be found at http://www.plantsci.cam.ac.uk/research/davidbaulcombe/methods/downloads/smallrna.pdf/view), with the following modifications: Cells were centrifuged and resuspended in 0.25 mL of water and mixed with 0.25 mL of Lysis buffer (50 mM Tris-HCl pH 8.0, 200 mM NaCl, 50 mM EDTA, 2% SDS, 1 mg/mL proteinase K). Lysis buffer was incubated at 50 °C for 5 min prior to mixing with cells. Cell suspension was then incubated at 25 °C for 20 min. Finally, 2 mL of PureZol (Biorad) was added and samples were snap-frozen. RNA quality was assessed in gel and quantified in Nanodrop (ThermoFisher scientific).

miRNA cleavage site determination was performed as previously described.[66] Briefly, 10 μg of total RNA was ligated with an RNA oligo (5′ CGACUGGAGCACGAGGACACUGACAUGGAC UGAAGGAGUAGAAA 3′) using T4 RNA ligase for 1 h at 37 °C. RNA was extracted with phenol/chloform and precipitated with ethanol and sodium acetate. The precipitated RNA was retrotranscribed into cDNA by SuperScript IV reverse transcriptase (ThermoFisher scientific), using random hexamers and following manufacturer's recommendations. Two microliters of the cDNA was used as template of a PCR using primers FJN456 (5′- CGACTGGAGCACGAGGACACTGA) and FJN495 (5′- TGGGGTAGGGGTGGGGGCCAG). A 2 μL portion of this PCR was used as template of a second PCR with primers FJN457 (5′-GGACACTGACATGGACTGAAGGAGTA) and FJN496 (5′- TGACCCAGTCGCGGATGGCCT). PCR was resolved in a 2% agarose gel and the specific band was isolated from the gel and cloned into pGEM-T easy (Promega) for sequencing.

Immuno-blotting. Chlamydomonas cells expressing FKB12 fusion proteins from liquid cultures were collected by centrifugation 4000*g* for 5 min at room temperature (RT), washed in 50 mM Tris-HCl pH 7.5, and resuspended in a minimal volume of the same solution. Cells were lysed by two cycles of slow freezing to −80 °C followed by thawing at RT. The soluble cell extract was separated from the insoluble fraction by centrifugation (15000*g* for 20 min at 4 °C). Total protein extracts (15 μg) were then subjected to 15% SDS-PAGE.

mCherry-expressing cells were harvested at 3500 rpm for 2 min (4 °C) and resuspended in 60 μL of DTT-carbonate buffer (0.1 M DTT, 0.1 M Na_2CO_3). After freezing at −20 °C and thawing, 55 μL of SDS-sucrose buffer were added (5% SDS, 30% sucrose). Samples were then boiled for 45 s at 95 °C, followed by 2 min incubation on ice and 13000*g* centrifugation for 2 min at RT. Protein extracts corresponding to 2 μg of chlorophyll were then separated using 12% SDS-PAGE.

For immunoblot analyses, proteins were then transferred to nitrocellulose membranes (Bio-Rad, 162-0115 or Amersham Protran). After blocking with 3 to 5% low-fat milk in PBS for 1 h at RT, membranes were incubated with primary antibody in 5% low-fat milk in PBS for 16 h at 4 °C. After four washes in PBS−0.1% tween-20 (TPBS), the membranes were incubated with secondary antibody in 5% low-fat milk in PBS for 1 h at RT, and subsequently washed four times in TPBS prior to chemiluminescence revelation using ECL. Primary antibodies used were anti-FKBP12[52] (1/5000 dilution; secondary was antirabbit 1/10000), anti-FLAG (Sigma-Aldrich F1804, 1/5000 dilution; secondary was antimouse 1/5000), anti-STREP (IBA, Catalog No. 2-1509-001, 1/5000 dilution; conjugated to HRP), anti-cMYC (Sigma-Aldrich M4439, 1/2500 dilution; secondary was antimouse 1/5000), anti-HA (Sigma-Aldrich H9658, 1/5000 dilution; secondary was antimouse 1/2500) and anti-PRPL1.[67] For mCherry serum, rabbits were immunized against purified full-length mCherry protein containing an N-terminal His_6-tag.

Microscopy. For mCherry experiments (Figure 6b−e), images were taken at 100× magnification with a BX53F microscope (Olympus). Fluorescence images for the detection of mCherry were taken using a TRITC filter. For other fluorescent proteins (Figure 6f−h), microscopy was performed as previously described.[7,68]

■ ASSOCIATED CONTENT

Supporting Information

The Supporting Information is available free of charge on the ACS Publications website at DOI: 10.1021/acssynbio.8b00251.

Additional figures as described in the text (PDF)

Supplemental tables as described in the text. All parts accession numbers and the corresponding references are listed in Supplementary Table 2 (XLSX)

■ AUTHOR INFORMATION

Corresponding Authors

*Tel.: +33 (0)628345239. Fax: +33 (0)158415025. E-mail: stephane.lemaire@ibpc.fr (S.D.L.).

*Tel.: +44 1223 333952. Fax: +44-1223-333953. E-mail: as25@cam.ac.uk (A.G.S.).

DOI: 10.1021/acssynbio.8b00251
ACS Synth. Biol. 2018, 7, 2074−2086

*Tel.: +49(0)631 205 2697. Fax: +49(0)631 205 2999. E-mail: schroda@bio.uni-kl.de (M.S.).

ORCID

Pierre Crozet: 0000-0001-5113-2407
Konstantinos Vavitsas: 0000-0002-6828-1000
Olaf Kruse: 0000-0001-9874-382X
Poul-Erik Jensen: 0000-0001-6524-7723
Alison G. Smith: 0000-0001-6511-5704

Present Address

□K.V.: Australian Institute for Bioengineering and Nanotechnology (AIBN), The University of Queensland, Australia.

Author Contributions

¶P.C., F.J.N., F.W., and P.M. contributed equally to the work. S.D.L, A.G.S, M.S., P.E.J., O.K., J.L.C., and G.P. created the consortium that led this study. P.C., F.J.N., F.W., P.M., D.C.B., G.P., J.L.C., O.K., P.E.J., M.S., A.G.S., and S.D.L. designed the study and wrote the manuscript. P.C., F.J.N., F.W., P.M., K.B., K.J.L., M.E.P.P., P.A., A.G.R., S.S.G., J.N., B.S., J.T., R.T., L.D.W., K.V., T.B., W.H., F.d.C., M.C., A.D., J.H., C.H.M., M.d.M., and K.S. designed parts, modules and devices, performed the experiments, and/or analyzed data.

Notes

The authors declare no competing financial interest.

■ ACKNOWLEDGMENTS

The authors would like to thank Karin Gries and Vincent Assoun for their technical help. This work was supported in part by Agence Nationale de la Recherche Grant ANR-17-CE05-0008 and LABEX DYNAMO ANR-LABX-011 (to P.C., A.D., F.d.C., J.H., C.H.M., M.d.M., K.S., M.C., and S.D.L.), by the DFG-funded TRR175 and FOR2092 (to F.W., B.S., J.N., J.T., L.W., R.T., and M.S.), by OpenPlant (BBSRC/EPSRC) (to F.J.N. and S.S.G.), by Ministerio de Economia y Competitividad Grants BFU2015-68216-P and BIO2015-74432-JIN (to J.L.C. and M.E.P.P.), by the VILLUM Foundation (Project no. 13363) (to P.E.J., K.B., K.V.), by the Technology Platforms at the Center for Biotechnology (CeBiTec) Bielefeld University (to K.L., T.B., and O.K.), by UK Biotechnology and Biological Sciences Research Council (BBSRC) (to P.M. and A.G.R.) and by ERA-SynBio project Sun2Chem (to P.A. and G.P.).

■ ABBREVIATION

MoClo,Modular Cloning; TU,Transcriptional Unit; RBCS2,Ribulose Bisphosphate Carboxylase Oxygenase small subunit 2; HSP70,Heat Shock Protein 70; AR,HSP70A/RBCS2; TUB2,Tubulin 2; PSAD,Photosystem I reaction center subunit II; HET,4-methyl-5-(2-hydroxyethyl) thiazole; HMP,4-amino-5-hydroxymethyl-2-methylpyrimidine; amiRNA,artificial micro RNA; TAP,Tris Acetate Phosphate

■ REFERENCES

(1) Zargar, A., Bailey, C. B., Haushalter, R. W., Eiben, C. B., Katz, L., and Keasling, J. D. (2017) Leveraging microbial biosynthetic pathways for the generation of 'drop-in' biofuels. *Curr. Opin. Biotechnol. 45*, 156−163.

(2) Georgianna, D. R., and Mayfield, S. P. (2012) Exploiting diversity and synthetic biology for the production of algal biofuels. *Nature 488*, 329−335.

(3) Wijffels, R. H., Kruse, O., and Hellingwerf, K. J. (2013) Potential of industrial biotechnology with cyanobacteria and eukaryotic microalgae. *Curr. Opin. Biotechnol. 24*, 405−413.

(4) Gimpel, J. A., Henríquez, V., and Mayfield, S. P. (2015) *Front. Microbiol. 6*, 1376.

(5) Scranton, M. A., Ostrand, J. T., Fields, F. J., and Mayfield, S. P. (2015) Chlamydomonas as a model for biofuels and bio-products production. *Plant J. 82*, 523−531.

(6) Gangl, D., Zedler, J. A., Rajakumar, P. D., Martinez, E. M., Riseley, A., Wlodarczyk, A., Purton, S., Sakuragi, Y., Howe, C. J., Jensen, P. E., and Robinson, C. (2015) Biotechnological exploitation of microalgae. *J. Exp. Bot. 66*, 6975−6990.

(7) Lauersen, K. J., Baier, T., Wichmann, J., Wordenweber, R., Mussgnug, J. H., Hubner, W., Huser, T., and Kruse, O. (2016) Efficient phototrophic production of a high-value sesquiterpenoid from the eukaryotic microalga Chlamydomonas reinhardtii. *Metab. Eng. 38*, 331−343.

(8) Wichmann, J., Baier, T., Wentnagel, E., Lauersen, K. J., and Kruse, O. (2017) Tailored carbon partitioning for phototrophic production of (E)-alpha-bisabolene from the green microalga Chlamydomonas reinhardtii. *Metab. Eng. 45*, 211.

(9) Merchant, S. S., Prochnik, S. E., Vallon, O., Harris, E. H., Karpowicz, S. J., Witman, G. B., Terry, A., Salamov, A., Fritz-Laylin, L. K., Marechal-Drouard, L., Marshall, W. F., Qu, L. H., Nelson, D. R., Sanderfoot, A. A., Spalding, M. H., Kapitonov, V. V., Ren, Q., Ferris, P., Lindquist, E., Shapiro, H., Lucas, S. M., Grimwood, J., Schmutz, J., Cardol, P., Cerutti, H., Chanfreau, G., Chen, C. L., Cognat, V., Croft, M. T., Dent, R., Dutcher, S., Fernandez, E., Fukuzawa, H., Gonzalez-Ballester, D., Gonzalez-Halphen, D., Hallmann, A., Hanikenne, M., Hippler, M., Inwood, W., Jabbari, K., Kalanon, M., Kuras, R., Lefebvre, P. A., Lemaire, S. D., Lobanov, A. V., Lohr, M., Manuell, A., Meier, I., Mets, L., Mittag, M., Mittelmeier, T., Moroney, J. V., Moseley, J., Napoli, C., Nedelcu, A. M., Niyogi, K., Novoselov, S. V., Paulsen, I. T., Pazour, G., Purton, S., Ral, J. P., Riano-Pachon, D. M., Riekhof, W., Rymarquis, L., Schroda, M., Stern, D., Umen, J., Willows, R., Wilson, N., Zimmer, S. L., Allmer, J., Balk, J., Bisova, K., Chen, C. J., Elias, M., Gendler, K., Hauser, C., Lamb, M. R., Ledford, H., Long, J. C., Minagawa, J., Page, M. D., Pan, J., Pootakham, W., Roje, S., Rose, A., Stahlberg, E., Terauchi, A. M., Yang, P., Ball, S., Bowler, C., Dieckmann, C. L., Gladyshev, V. N., Green, P., Jorgensen, R., Mayfield, S., Mueller-Roeber, B., Rajamani, S., Sayre, R. T., Brokstein, P., Dubchak, I., Goodstein, D., Hornick, L., Huang, Y. W., Jhaveri, J., Luo, Y., Martinez, D., Ngau, W. C., Otillar, B., Poliakov, A., Porter, A., Szajkowski, L., Werner, G., Zhou, K., Grigoriev, I. V., Rokhsar, D. S., and Grossman, A. R. (2007) The Chlamydomonas genome reveals the evolution of key animal and plant functions. *Science 318*, 245−250.

(10) Gallaher, S. D., Fitz-Gibbon, S. T., Glaesener, A. G., Pellegrini, M., and Merchant, S. S. (2015) Chlamydomonas Genome Resource for Laboratory Strains Reveals a Mosaic of Sequence Variation, Identifies True Strain Histories, and Enables Strain-Specific Studies. *Plant Cell 27*, 2335−2352.

(11) Scaife, M. A., Nguyen, G. T., Rico, J., Lambert, D., Helliwell, K. E., and Smith, A. G. (2015) Establishing Chlamydomonas reinhardtii as an industrial biotechnology host. *Plant J. 82*, 532−546.

(12) Li, X., Zhang, R., Patena, W., Gang, S. S., Blum, S. R., Ivanova, N., Yue, R., Robertson, J. M., Lefebvre, P. A., Fitz-Gibbon, S. T., Grossman, A. R., and Jonikas, M. C. (2016) An Indexed, Mapped Mutant Library Enables Reverse Genetics Studies of Biological Processes in Chlamydomonas reinhardtii. *Plant Cell 28*, 367−387.

(13) Jinkerson, R. E., and Jonikas, M. C. (2015) Molecular techniques to interrogate and edit the Chlamydomonas nuclear genome. *Plant J. 82*, 393−412.

(14) Agapakis, C. M., Boyle, P. M., and Silver, P. A. (2012) Natural strategies for the spatial optimization of metabolism in synthetic biology. *Nat. Chem. Biol. 8*, 527−535.

(15) Chen, A. H., and Silver, P. A. (2012) Designing biological compartmentalization. *Trends Cell Biol. 22*, 662−670.

(16) Barahimipour, R., Neupert, J., and Bock, R. (2016) Efficient expression of nuclear transgenes in the green alga Chlamydomonas: synthesis of an HIV antigen and development of a new selectable marker. *Plant Mol. Biol. 90*, 403−418.

DOI: 10.1021/acssynbio.8b00251
ACS Synth. Biol. 2018, 7, 2074−2086

(17) Rasala, B. A., Lee, P. A., Shen, Z., Briggs, S. P., Mendez, M., and Mayfield, S. P. (2012) Robust expression and secretion of Xylanase1 in Chlamydomonas reinhardtii by fusion to a selection gene and processing with the FMDV 2A peptide. *PLoS One 7*, e43349.
(18) Scaife, M. A., and Smith, A. G. (2016) Towards developing algal synthetic biology. *Biochem. Soc. Trans. 44*, 716−722.
(19) Endy, D. (2011) Building a new biology. *C. R. Chim. 14*, 424−428.
(20) Casini, A., Storch, M., Baldwin, G. S., and Ellis, T. (2015) Bricks and blueprints: methods and standards for DNA assembly. *Nat. Rev. Mol. Cell Biol. 16*, 568−576.
(21) Engler, C., Kandzia, R., and Marillonnet, S. (2008) A one pot, one step, precision cloning method with high throughput capability. *PLoS One 3*, e3647.
(22) Weber, E., Engler, C., Gruetzner, R., Werner, S., and Marillonnet, S. (2011) A modular cloning system for standardized assembly of multigene constructs. *PLoS One 6*, e16765.
(23) Smanski, M. J., Bhatia, S., Zhao, D., Park, Y., Woodruff, B. A. L., Giannoukos, G., Ciulla, D., Busby, M., Calderon, J., Nicol, R., Gordon, D. B., Densmore, D., and Voigt, C. A. (2014) Functional optimization of gene clusters by combinatorial design and assembly. *Nat. Biotechnol. 32*, 1241−1249.
(24) Celinska, E., Ledesma-Amaro, R., Larroude, M., Rossignol, T., Pauthenier, C., and Nicaud, J. M. (2017) Golden Gate Assembly system dedicated to complex pathway manipulation in Yarrowia lipolytica. *Microb. Biotechnol. 10*, 450−455.
(25) Engler, C., Youles, M., Gruetzner, R., Ehnert, T. M., Werner, S., Jones, J. D., Patron, N. J., and Marillonnet, S. (2014) A golden gate modular cloning toolbox for plants. *ACS Synth. Biol. 3*, 839−843.
(26) Iverson, S. V., Haddock, T. L., Beal, J., and Densmore, D. M. (2016) CIDAR MoClo: Improved MoClo Assembly Standard and New E. coli Part Library Enable Rapid Combinatorial Design for Synthetic and Traditional Biology. *ACS Synth. Biol. 5*, 99−103.
(27) Lee, M. E., DeLoache, W. C., Cervantes, B., and Dueber, J. E. (2015) A Highly Characterized Yeast Toolkit for Modular, Multipart Assembly. *ACS Synth. Biol. 4*, 975−986.
(28) Martella, A., Matjusaitis, M., Auxillos, J., Pollard, S. M., and Cai, Y. (2017) EMMA: An Extensible Mammalian Modular Assembly Toolkit for the Rapid Design and Production of Diverse Expression Vectors. *ACS Synth. Biol. 6*, 1380.
(29) Moore, S. J., Lai, H. E., Kelwick, R. J., Chee, S. M., Bell, D. J., Polizzi, K. M., and Freemont, P. S. (2016) EcoFlex: A Multifunctional MoClo Kit for E. coli Synthetic Biology. *ACS Synth. Biol. 5*, 1059−1069.
(30) Patron, N. J., Orzaez, D., Marillonnet, S., Warzecha, H., Matthewman, C., Youles, M., Raitskin, O., Leveau, A., Farre, G., Rogers, C., Smith, A., Hibberd, J., Webb, A. A., Locke, J., Schornack, S., Ajioka, J., Baulcombe, D. C., Zipfel, C., Kamoun, S., Jones, J. D., Kuhn, H., Robatzek, S., Van Esse, H. P., Sanders, D., Oldroyd, G., Martin, C., Field, R., O'Connor, S., Fox, S., Wulff, B., Miller, B., Breakspear, A., Radhakrishnan, G., Delaux, P. M., Loque, D., Granell, A., Tissier, A., Shih, P., Brutnell, T. P., Quick, W. P., Rischer, H., Fraser, P. D., Aharoni, A., Raines, C., South, P. F., Ane, J. M., Hamberger, B. R., Langdale, J., Stougaard, J., Bouwmeester, H., Udvardi, M., Murray, J. A., Ntoukakis, V., Schafer, P., Denby, K., Edwards, K. J., Osbourn, A., and Haseloff, J. (2015) Standards for plant synthetic biology: a common syntax for exchange of DNA parts. *New Phytol. 208*, 13−19.
(31) Lopez-Paz, C., Liu, D., Geng, S., and Umen, J. G. (2017) Identification of Chlamydomonas reinhardtii endogenous genic flanking sequences for improved transgene expression. *Plant J. 92*, 1232−1244.
(32) Plucinak, T. M., Horken, K. M., Jiang, W., Fostvedt, J., Nguyen, S. T., and Weeks, D. P. (2015) Improved and versatile viral 2A platforms for dependable and inducible high-level expression of dicistronic nuclear genes in Chlamydomonas reinhardtii. *Plant J. 82*, 717−729.
(33) Lumbreras, V., Stevens, D. R., and Purton, S. (1998) Efficient foreign gene expression in Chlamydomonas reinhardtii mediated by an endogenous intron. *Plant J. 14*, 441−447.
(34) Strenkert, D., Schmollinger, S., and Schroda, M. (2013) Heat shock factor 1 counteracts epigenetic silencing of nuclear transgenes in Chlamydomonas reinhardtii. *Nucleic Acids Res. 41*, 5273−5289.
(35) Neupert, J., Karcher, D., and Bock, R. (2009) Generation of Chlamydomonas strains that efficiently express nuclear transgenes. *Plant J. 57*, 1140−1150.
(36) Schroda, M., Beck, C. F., and Vallon, O. (2002) Sequence elements within an HSP70 promoter counteract transcriptional transgene silencing in Chlamydomonas. *Plant J. 31*, 445−455.
(37) Eichler-Stahlberg, A., Weisheit, W., Ruecker, O., and Heitzer, M. (2009) Strategies to facilitate transgene expression in Chlamydomonas reinhardtii. *Planta 229*, 873−883.
(38) Shao, N., and Bock, R. (2008) A codon-optimized luciferase from Gaussia princeps facilitates the in vivo monitoring of gene expression in the model alga Chlamydomonas reinhardtii. *Curr. Genet. 53*, 381−388.
(39) Hall, M. P., Unch, J., Binkowski, B. F., Valley, M. P., Butler, B. L., Wood, M. G., Otto, P., Zimmerman, K., Vidugiris, G., Machleidt, T., Robers, M. B., Benink, H. A., Eggers, C. T., Slater, M. R., Meisenheimer, P. L., Klaubert, D. H., Fan, F., Encell, L. P., and Wood, K. V. (2012) Engineered luciferase reporter from a deep sea shrimp utilizing a novel imidazopyrazinone substrate. *ACS Chem. Biol. 7*, 1848−1857.
(40) Lodha, M., Schulz-Raffelt, M., and Schroda, M. (2008) A new assay for promoter analysis in Chlamydomonas reveals roles for heat shock elements and the TATA box in HSP70A promoter-mediated activation of transgene expression. *Eukaryotic Cell 7*, 172−176.
(41) Barahimipour, R., Strenkert, D., Neupert, J., Schroda, M., Merchant, S. S., and Bock, R. (2015) Dissecting the contributions of GC content and codon usage to gene expression in the model alga Chlamydomonas reinhardtii. *Plant J. 84*, 704−717.
(42) Best, R. J., Lyczakowski, J. J., Abalde-Cela, S., Yu, Z., Abell, C., and Smith, A. G. (2016) Label-Free Analysis and Sorting of Microalgae and Cyanobacteria in Microdroplets by Intrinsic Chlorophyll Fluorescence for the Identification of Fast Growing Strains. *Anal. Chem. 88*, 10445−10451.
(43) Ohresser, M., Matagne, R. F., and Loppes, R. (1997) Expression of the arylsulphatase reporter gene under the control of the nit1 promoter in Chlamydomonas reinhardtii. *Curr. Genet. 31*, 264−271.
(44) Schmollinger, S., Strenkert, D., and Schroda, M. (2010) An inducible artificial microRNA system for Chlamydomonas reinhardtii confirms a key role for heat shock factor 1 in regulating thermotolerance. *Curr. Genet. 56*, 383−389.
(45) Helliwell, K. E., Scaife, M. A., Sasso, S., Araujo, A. P., Purton, S., and Smith, A. G. (2014) Unraveling vitamin B12-responsive gene regulation in algae. *Plant Physiol. 165*, 388−397.
(46) Boudreau, E., Nickelsen, J., Lemaire, S. D., Ossenbuhl, F., and Rochaix, J. D. (2000) The Nac2 gene of Chlamydomonas encodes a chloroplast TPR-like protein involved in psbD mRNA stability. *EMBO J. 19*, 3366−3376.
(47) Croft, M. T., Moulin, M., Webb, M. E., and Smith, A. G. (2007) Thiamine biosynthesis in algae is regulated by riboswitches. *Proc. Natl. Acad. Sci. U. S. A. 104*, 20770−20775.
(48) Moulin, M., Nguyen, G. T., Scaife, M. A., Smith, A. G., and Fitzpatrick, T. B. (2013) Analysis of Chlamydomonas thiamin metabolism in vivo reveals riboswitch plasticity. *Proc. Natl. Acad. Sci. U. S. A. 110*, 14622−14627.
(49) Molnar, A., Schwach, F., Studholme, D. J., Thuenemann, E. C., and Baulcombe, D. C. (2007) miRNAs control gene expression in the single-cell alga Chlamydomonas reinhardtii. *Nature 447*, 1126−1129.
(50) Palombella, A. L., and Dutcher, S. K. (1998) Identification of the gene encoding the tryptophan synthase beta-subunit from Chlamydomonas reinhardtii. *Plant Physiol. 117*, 455−464.
(51) Young, C. L., Britton, Z. T., and Robinson, A. S. (2012) Recombinant protein expression and purification: a comprehensive

DOI: 10.1021/acssynbio.8b00251
ACS Synth. Biol. 2018, 7, 2074−2086

review of affinity tags and microbial applications. *Biotechnol. J. 7*, 620−634.
(52) Crespo, J. L., Diaz-Troya, S., and Florencio, F. J. (2005) Inhibition of target of rapamycin signaling by rapamycin in the unicellular green alga Chlamydomonas reinhardtii. *Plant Physiol. 139*, 1736−1749.
(53) Crivat, G., and Taraska, J. W. (2012) Imaging proteins inside cells with fluorescent tags. *Trends Biotechnol. 30*, 8−16.
(54) Engler, C., Gruetzner, R., Kandzia, R., and Marillonnet, S. (2009) Golden gate shuffling: a one-pot DNA shuffling method based on type IIs restriction enzymes. *PLoS One 4*, e5553.
(55) Greiner, A., Kelterborn, S., Evers, H., Kreimer, G., Sizova, I., and Hegemann, P. (2017) Targeting of Photoreceptor Genes in Chlamydomonas reinhardtii via Zinc-finger Nucleases and CRISPR/Cas9. *Plant Cell 29*, 2498.
(56) Sizova, I., Greiner, A., Awasthi, M., Kateriya, S., and Hegemann, P. (2013) Nuclear gene targeting in Chlamydomonas using engineered zinc-finger nucleases. *Plant J. 73*, 873−882.
(57) Shin, S. E., Lim, J. M., Koh, H. G., Kim, E. K., Kang, N. K., Jeon, S., Kwon, S., Shin, W. S., Lee, B., Hwangbo, K., Kim, J., Ye, S. H., Yun, J. Y., Seo, H., Oh, H. M., Kim, K. J., Kim, J. S., Jeong, W. J., Chang, Y. K., and Jeong, B. R. (2016) CRISPR/Cas9-induced knockout and knock-in mutations in Chlamydomonas reinhardtii. *Sci. Rep. 6*, 27810.
(58) Baek, K., Kim, D. H., Jeong, J., Sim, S. J., Melis, A., Kim, J. S., Jin, E., and Bae, S. (2016) DNA-free two-gene knockout in Chlamydomonas reinhardtii via CRISPR-Cas9 ribonucleoproteins. *Sci. Rep. 6*, 30620.
(59) Ferenczi, A., Pyott, D. E., Xipnitou, A., and Molnar, A. (2017) Efficient targeted DNA editing and replacement in Chlamydomonas reinhardtii using Cpf1 ribonucleoproteins and single-stranded DNA. *Proc. Natl. Acad. Sci. U. S. A. 114*, 13567−13572.
(60) Doron, L., Segal, N., and Shapira, M. (2016) Transgene Expression in Microalgae-From Tools to Applications. *Front. Plant Sci. 7*, 505.
(61) Sager, R. (1955) Inheritance in the Green Alga Chlamydomonas Reinhardi. *Genetics 40*, 476−489.
(62) Kuchka, M. R., Goldschmidt-Clermont, M., van Dillewijn, J., and Rochaix, J. D. (1989) Mutation at the Chlamydomonas nuclear NAC2 locus specifically affects stability of the chloroplast psbD transcript encoding polypeptide D2 of PS II. *Cell 58*, 869−876.
(63) Gorman, D. S., and Levine, R. P. (1965) Cytochrome f and plastocyanin: their sequence in the photosynthetic electron transport chain of Chlamydomonas reinhardi. *Proc. Natl. Acad. Sci. U. S. A. 54*, 1665−1669.
(64) Kindle, K. L. (1990) High-frequency nuclear transformation of Chlamydomonas reinhardtii. *Proc. Natl. Acad. Sci. U. S. A. 87*, 1228−1232.
(65) Molnar, A., Bassett, A., Thuenemann, E., Schwach, F., Karkare, S., Ossowski, S., Weigel, D., and Baulcombe, D. (2009) Highly specific gene silencing by artificial microRNAs in the unicellular alga Chlamydomonas reinhardtii. *Plant J. 58*, 165−174.
(66) Llave, C., Xie, Z., Kasschau, K. D., and Carrington, J. C. (2002) Cleavage of Scarecrow-like mRNA targets directed by a class of Arabidopsis miRNA. *Science 297*, 2053−2056.
(67) Ries, F., Carius, Y., Rohr, M., Gries, K., Keller, S., Lancaster, C. R. D., and Willmund, F. (2017) Structural and molecular comparison of bacterial and eukaryotic trigger factors. *Sci. Rep. 7*, 10680.
(68) Lauersen, K. J., Kruse, O., and Mussgnug, J. H. (2015) Targeted expression of nuclear transgenes in Chlamydomonas reinhardtii with a versatile, modular vector toolkit. *Appl. Microbiol. Biotechnol. 99*, 3491−3503.
(69) Roehner, N., Beal, J., Clancy, K., Bartley, B., Misirli, G., Grunberg, R., Oberortner, E., Pocock, M., Bissell, M., Madsen, C., Nguyen, T., Zhang, M., Zhang, Z., Zundel, Z., Densmore, D., Gennari, J. H., Wipat, A., Sauro, H. M., and Myers, C. J. (2016) Sharing Structure and Function in Biological Design with SBOL 2.0. *ACS Synth. Biol. 5*, 498−506.

DOI: 10.1021/acssynbio.8b00251
ACS Synth. Biol. 2018, 7, 2074−2086